

## Mechanistic study of copper-catalyzed intramolecular *ortho*-C–H activation/carbon-nitrogen and carbon-oxygen cyclizations

TANG ShiYa, GONG TianJun & FU Yao\*

Department of Chemistry, University of Science and Technology of China, Hefei 230026, China

Received August 4, 2012; accepted August 27, 2012; published online November 28, 2012

Intramolecular *ortho*-C–H activation and C–N/C–O cyclizations of phenyl amidines and amides have recently been achieved under Cu catalysis. These reactions provide important examples of Cu-catalyzed functionalization of inert C–H bonds, but their mechanisms remain poorly understood. In the present study the several possible mechanisms including electrophilic aromatic substitution, concerted metalation-deprotonation (CMD), Friedel-Crafts mechanism, radical mechanism, and proton-coupled electron transfer have been theoretically examined. Cu(II)-assisted CMD mechanism is found to be the most feasible for both C–O and C–N cyclizations. This mechanism includes three steps, i.e. CMD with Cu(II), oxidation of the Cu(II) intermediate, and reductive elimination from Cu(III). Our calculations show that Cu(II) mediates the C–H activation through an six-membered ring CMD transition state similar to that proposed for many Pd-catalyzed C–H activation reactions. It is also interesting to find that the rate-limiting steps are different for C–N and C–O cyclizations: for the former it is concerted metalation-deprotonation with Cu(II), whereas for the latter it is reductive elimination from Cu(III). The above conclusions are consistent with the experimental kinetic isotope effects (1.0 and 2.1 for C–O and C–N cyclizations, respectively), substituent effects, and the reactions under O<sub>2</sub>-free conditions.

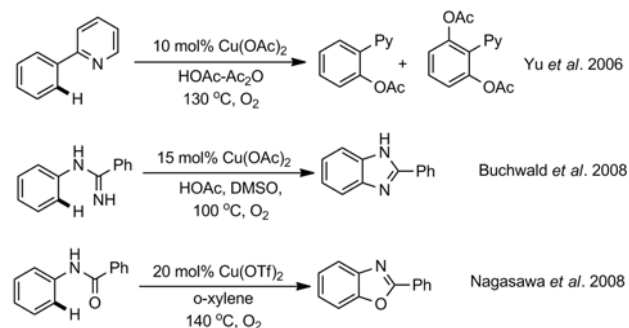
**mechanism, DFT, copper, C–H activation, concerted metalation-deprotonation**

### 1 Introduction

Transition metal-catalyzed C–H activation has emerged as a powerful method in synthetic organic chemistry [1]. Such reactions promoted by Rh- [2], Ru- [3], and Pd-catalysts [4] have been extensively studied, but Cu-catalyzed C–H activation began to draw attentions as a complementary method only recently [5]. In this area, much work has been directed to the Cu-catalyzed functionalization of acidic C–H bonds as triggered by base [6], whereas base-free activation of inert C–H bonds by Cu catalysts has been less studied. In 2006 Yu *et al.* reported Cu(OAc)<sub>2</sub>-catalyzed intermolecular C–H functionalization (Scheme 1) [7]. Later, Buchwald *et al.* reported Cu(OAc)<sub>2</sub>-catalyzed *ortho*-C–H activation/C–N cyclization of amidines [8], while Nagasawa *et al.* reported

Cu(OTf)<sub>2</sub>-catalyzed *ortho*-C–H activation/C–O cyclization of amides [9].

Despite the great contemporary interest in Cu-catalyzed C–H activation, it remains unclear how these reactions take place. For Cu(OAc)<sub>2</sub>-catalyzed pyridine-directed C–H activation

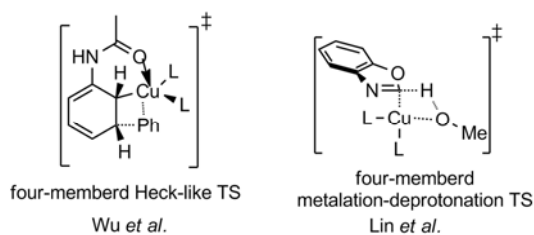


**Scheme 1** Representative examples for Cu-catalyzed activation of inert C–H bonds.

\*Corresponding author (email: fuyao@ustc.edu.cn)

vation, Yu *et al.* proposed a single electron transfer process involving a cation-radical intermediate [7, 10]. On the other hand, both Buchwald and Nagasawa suggested an electrophilic attack mechanism in their C–N and C–O cyclization reactions [8, 9]. Even so, the electrophilic attack may occur at either Cu or Cu-coordinated nitrogen/oxygen atoms [5, 8]. Furthermore, although Wang [11] and Stahl [12] identified macrocyclic aryl–Cu(III) complexes in some model C–H activation processes [11], it is unclear whether Cu(III) is still involved for the reactions without macrocyclic ligands [8, 9, 13]. Finally, very few theoretical studies have been carried out on Cu-catalyzed C–H activation [14]. Wu *et al.* proposed a Heck-like transition state for Cu-mediated *meta*-C–H functionalization, whereas Lin *et al.* proposed a four-membered concerted metalation–deprotonation transition state for the coupling of Ar–H with PhI (Scheme 2) [14]. These theoretical results may only be applied to intermolecular reactions, because neither the Heck-like nor the four-membered concerted metalation–deprotonation transition state appears possible for intramolecular reactions due to the skeleton restraint.

In an attempt to elucidate the mechanism, we have carried out a thorough theoretical study of Cu-catalyzed *ortho*-C–H activation/C–N and C–O cyclization reactions. Several possible pathways are examined (Scheme 3) [5b, 8, 9]. In mechanism A, the N- or O-bound Cu atom in the Cu-coordinated complex **2** attacks the aromatic ring to generate a Wheland intermediate **3**, which then undergoes aromatization and reductive elimination to give the product **9**. This mechanism involves stepwise metalation and deprotonation. Different from mechanism A, mechanism B involves a concerted metalation and deprotonation to form an aryl–Cu complex **4** instead of a Wheland intermediate. Such a process is similar to that proposed for Pd-catalyzed C–H activation [15]. In mechanism C, the Cu-bound N or O atom in **2** attacks the aromatic ring to form **5** with concerted release of a reduced Cu species, followed by re-aromatization to provide **9**. Mechanism A and C were both mentioned for the benzimidazole-forming process in Buchwald's work [8]. Moreover, mechanisms A and C may also proceed in a radical manner (i.e. mechanisms D and E) [5]. In mechanisms D and E, a single electron transfer from the aromatic ring to the coordinated Cu(II) takes place to generate a radical cation intermediate **6** [7]. The following steps occur in a similar



**Scheme 2** Previously proposed transition states for Cu-catalyzed C–H activation.

way as that in mechanisms A and C. None of the above mechanisms can be excluded by the available experimental data. In addition, two specific details of these mechanisms remain unknown, namely (1) which step is rate-determining, and (2) is the oxidation state of the key Cu intermediate +2 or +3?

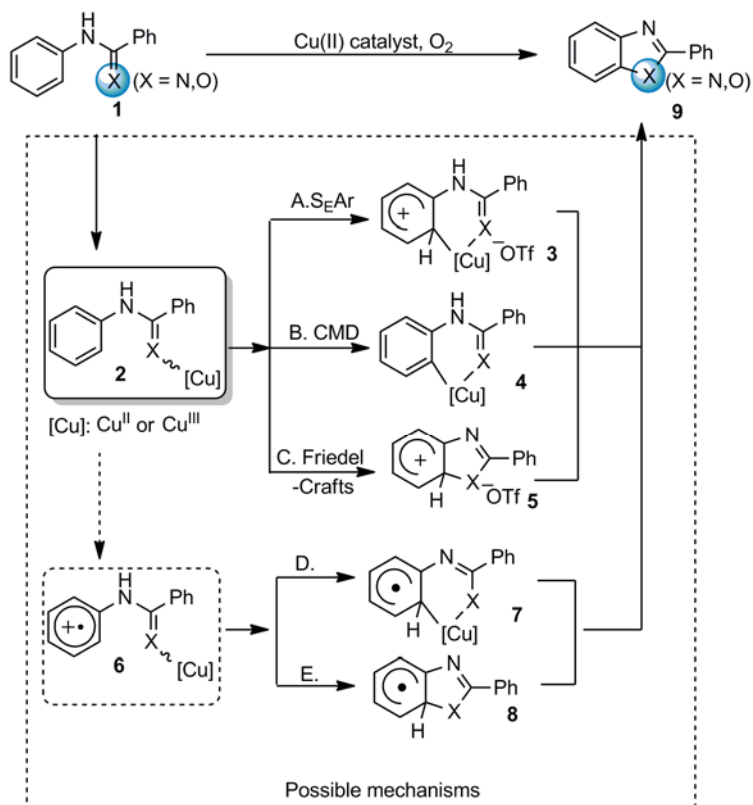
Here mechanisms A, B and C with Cu in either +2 or +3 oxidation state are examined. Our results indicate that the mechanism B (concerted metalation–deprotonation, CMD) is energetically favored for Cu-catalyzed intramolecular C–H activation/C–N and C–O cyclizations. It consists of three steps, i.e. concerted metalation–deprotonation with Cu(II), oxidation of the Cu(II) intermediate, and reductive elimination from Cu(III). Importantly, it is Cu(II) that mediates the C–H activation through an acetate/trifluoromethanesulfonate (triflate)(OAc/OTf)-assisted CMD process. Moreover, while reductive elimination is the rate-limiting step for C–O cyclization, CMD is the rate-limiting step for C–N cyclization. The theoretical mechanism is consistent with the experimental kinetic isotope effects and substituent effects. We further investigated the radical pathways (mechanisms D and E) and proton-coupled electron transfer. According to the radical scavenger experiment and related calculations, we found that neither the radical pathway nor proton-coupled electron transfer was plausible in the C–O and C–N cyclization reactions.

## 2 Calculations of different mechanisms

### 2.1 Mechanisms A, B and C for C–O cyclization

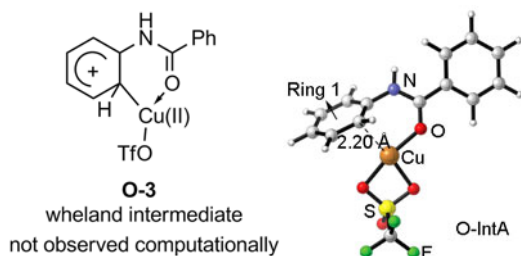
#### 2.1.1 Problem with mechanism A

Mechanism A (i.e. electrophilic aromatic substitution,  $S_EAr$ ) has previously been proposed for Cu-catalyzed C–H functionalization by Buchwald and Nagasawa *et al.*, because they found that the related reaction with an electron-donating substituent ( $R = OMe$ ) is faster than that with an electron-withdrawing group ( $R = Cl$  or  $COOMe$ ) [8, 9]. However, with the help of pulse electron paramagnetic resonance (EPR) methods in combination with density functional theory (DFT) calculations, Ribas *et al.* precluded the Wheland intermediate (the core of  $S_EAr$  mechanism) in the Cu-catalyzed C–H cleavage reaction [10]. In the present study, we employed the electrophilic cationic Cu(II) species to investigate the  $S_EAr$  pathway which involved the important intermediate **O-3** (shown in Schemes 1 and 4). However, all attempts resulted in the structure of **O-IntA**. To examine whether or not **O-IntA** is a Wheland intermediate, we tested the aromaticity of Ring1 in **O-IntA** by the harmonic oscillator model of aromaticity (HOMA) index [16] and the nucleus-independent chemical shift (NICS) index [17]. The reason for this is that significant loss of aromaticity is a critical character of Wheland intermediate. As a structure-based measure of aromaticity, HOMA indexes were 0.968 and 0.994 for **O-IntA** and the amide, re-



$S_EAr$  means electrophilic aromatic substitution; CMD means concerted metalation-deprotonation

**Scheme 3** Possible mechanisms for Cu-catalyzed *ortho*-C–H activation/C–N and C–O cyclizations.



**Scheme 4** Related intermediate in mechanism A.

spectively. As a magnetic measure of aromaticity, the NICS(1) indexes were  $-8.69$  and  $-10.16$  ppm for **O-IntA** and the amide, respectively. These data both indicated that the aromaticity of Ring1 in **O-IntA** does not decrease significantly as compared to the substrate amide [10]. Therefore, **O-IntA** is not a Wheland intermediate. Without the existence of the key Wheland intermediate (**O-3**), the  $S_EAr$  mechanism does not appear possible in Cu-catalyzed intramolecular cyclization.

### 2.1.2 Concerted metalation–deprotonation mechanism

Mechanism B (i.e. the CMD mechanism) is often proposed for transition metal-catalyzed C–H activation [1]. This mechanism consists of three main steps: (i) metal coordina-

tion; (ii) concerted metalation–deprotonation; (iii) reductive elimination and catalyst regeneration. Cu has two possible oxidation states, i.e. Cu(II) and Cu(III). Therefore, we have to examine both oxidation states for the CMD mechanism as shown below.

(i) CMD of Cu(III) intermediate. Cu(III) intermediates are commonly proposed for Cu-catalyzed Ullmann reactions [13, 18]. Recently, Stahl *et al.* proposed that Cu(III) species may be involved in some Cu-catalyzed intramolecular *ortho*-C–H activation [5, 19]. For the present reaction, we propose that  $Cu(OTf)_2$  first coordinates to the O atom of the reactant 1 to give a Cu(II) complex **O-Int1** [20] (exergonic,  $-13.8$  kcal/mol, Figures 1 and 2). Subsequently, **O-Int1** is oxidized by another molecule of  $Cu(OTf)_2$  to give a Cu(III) intermediate **O/CMD-Int1-III**. Note that a similar disproportionation reaction of Cu(II) salts was previously described by Ribas and Stahl *et al.* [21]. With the help of triflate, the Cu(III) atom of **O/CMD-Int1-III** reacts with the N-phenyl ring through a six-membered-ring transition state **O/CMD-TS12-III**. The activation energy for this transition state is  $+42.1$  kcal/mol as calculated from **O-Int1** to **O/CMD-TS12-III**. Because **O/CMD-TS12-III** corresponds to the breaking of the C–H bond and concerted formation of the H–O and Cu–C bonds, this process can be considered as a CMD process [15]. An aryl–Cu(III) [5, 12, 22] complex is

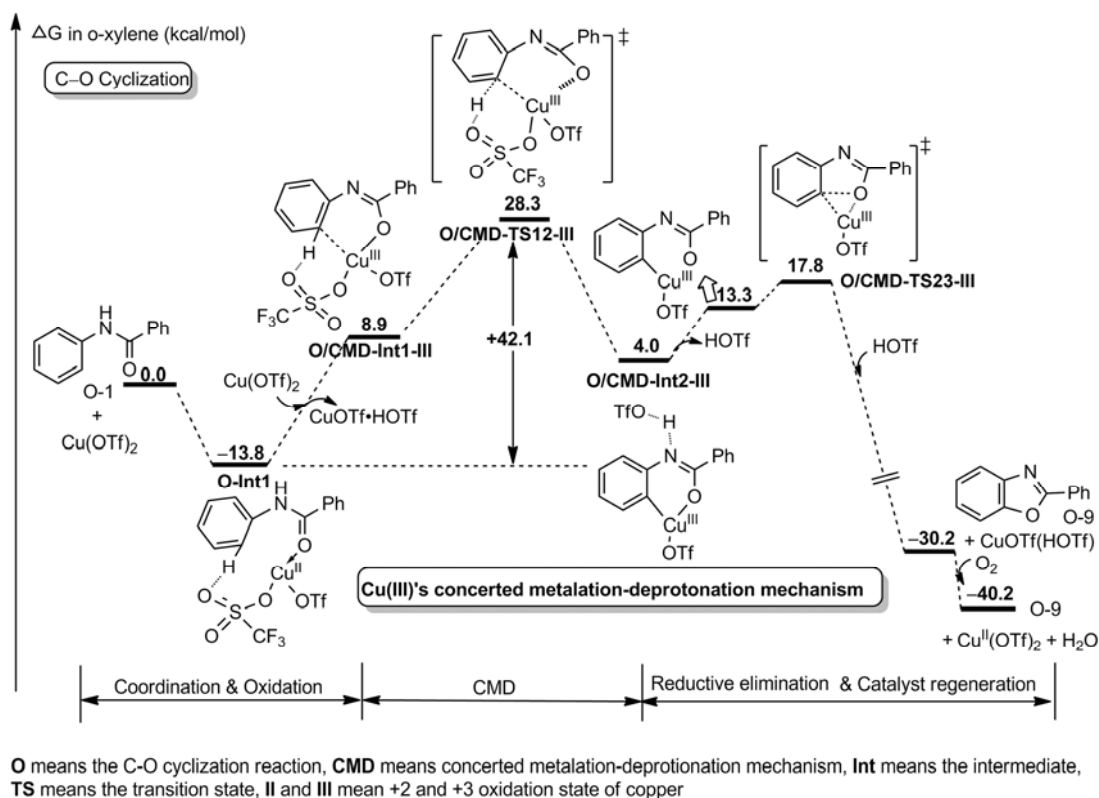


**Figure 1** Cu(III)-assisted concerted metalation-deprotonation mechanism for C-O formation.

generated in the CMD process, which can easily undergo reductive elimination to give the target product with a low activation energy of +13.8 kcal/mol. After reductive elimination, the product and reduced Cu(I) species are formed. With the aid of  $O_2$ , the Cu(I) species is easily re-oxidized to Cu(II) to finish the catalytic cycle.

The rate-determining step of the above pathway is the concerted metalation-deprotonation process with an overall barrier of +42.1 kcal/mol (Figure 1). This barrier is too high for the reaction to proceed at the reported temperature (i.e. 140 °C). Therefore, the Cu(III)-assisted CMD mechanism does not appear to be favored.

(ii) CMD of Cu(II) intermediate. This pathway also starts from the Cu(II) complex **O-Int1**. However, instead of being oxidized to Cu(III), the Cu(II) metal center attacks the N-phenyl ring directly and at the same time the triflate anion coordinated with Cu(II) abstracts the proton from the aryl ring (Figures 3 and 4). This process proceeds via a cyclic six-membered ring transition state **O/CMD-TS12-II** involving breaking of the C-H bond (1.42 Å) and concerted formation of the H-O (1.20 Å) and Cu-C (2.02 Å) bonds. Evidently this process is also a CMD process, but its activation energy is calculated to be as low as +20.9 kcal/mol (from **O-Int1** to **O/CMD-TS12-II**). A new four-coordinated Cu(II) intermediate **O/CMD-Int2-II** is generated through the CMD process. This intermediate has two pathways to finish

the catalytic cycle (Figure 2).

Pathway 1: direct reductive elimination (unfavorable). The Cu(II) intermediate **O/CMD-Int2-II** may directly undergo reductive elimination to afford the product via a three-center transition state **O/CMD-TS23-II**. Meanwhile, a Cu(0) species is generated and will be converted to the initial Cu(II) catalyst with the aid of  $O_2$ . Unfortunately, this reductive elimination is calculated to be a very difficult process with a high activation energy (+50.1 kcal/mol).

Pathway 2: oxidation and reductive elimination (favorable). Alternatively **O/CMD-Int2-II** may be oxidized by another molecule of  $Cu(OTf)_2$  to produce a four-coordinated Cu(III) intermediate **O/CMD-Int3-III** (Note: **O/CMD-Int3-III** is also involved in the Cu(III)-assisted CMD process). Our calculation shows that this oxidation is only slightly endergonic by +2.8 kcal/mol. Subsequently, **O/CMD-Int2-III** can undergo reductive elimination easily to give the product **O-9** with a lower activation energy (+31.6 kcal/mol).

By comparing the above two pathways (Figure 2), we conclude that the Cu(II)-assisted CMD mechanism should involve three steps: concerted metalation-deprotonation with Cu(II), oxidation of Cu(II) intermediate, and reductive elimination from Cu(III). Reductive elimination is the rate-limiting step and the overall barrier of +31.6 kcal/mol. Evidently Cu(II)-assisted CMD mechanism is more favora-

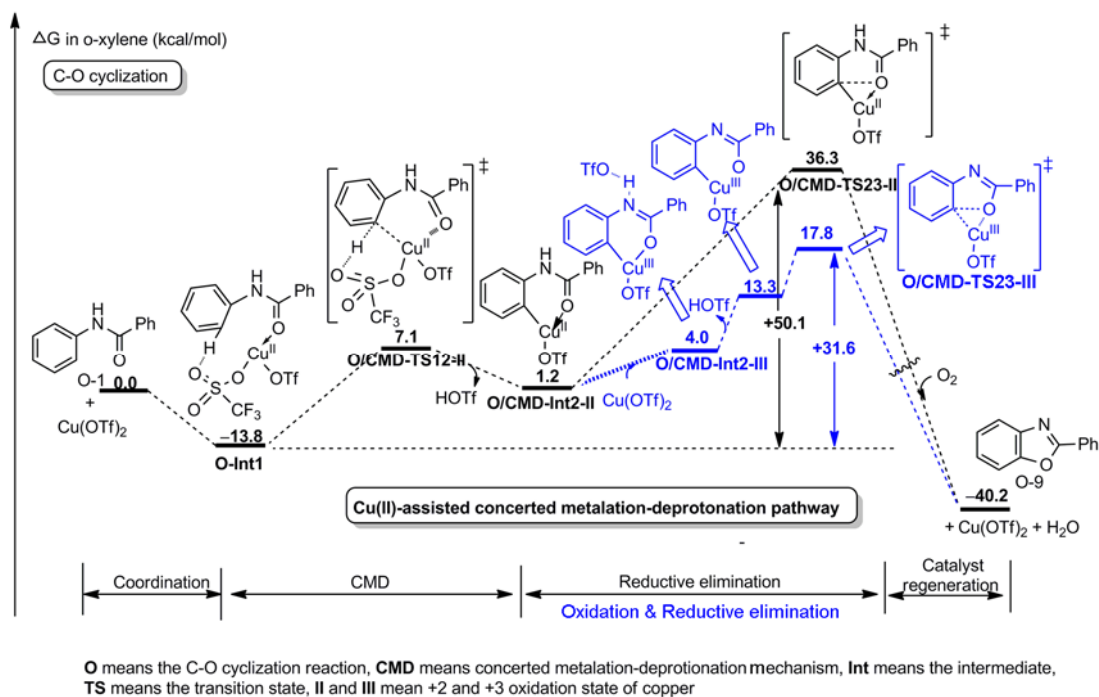


**Figure 2** Cu(II)-assisted concerted metalation–deprotonation pathway for C–O formation.

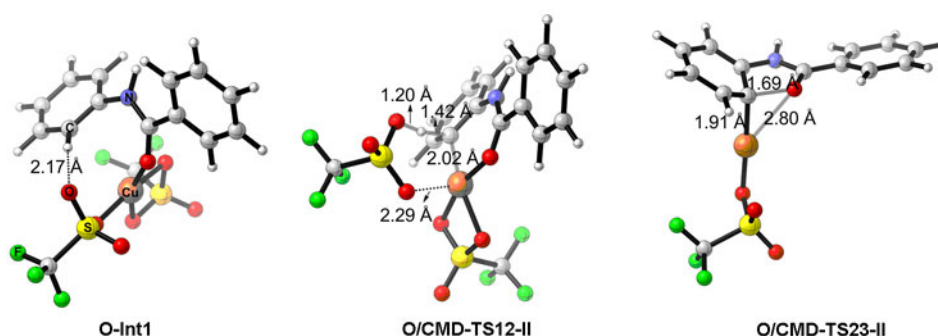


**Figure 3** Important structures in Cu(II)-assisted concerted metalation–deprotonation pathway for C–O formation.

ble than its Cu(III) counterpart.

### 2.1.3 Friedel-Crafts mechanism

An alternative pathway to provide the C–H functionalization products is Lewis acid-catalyzed Friedel-Crafts mechanism (i.e. mechanism C) [23, 24]. With this mechanism the reaction is proposed to include three steps: (i) metal coordination; (ii) electrophilic substitution of Cu-bound O atom; (iii) deprotonation and catalyst regeneration. Different from the CMD mechanism, electrophilic attack and deprotonation are separated steps in mechanism C.

(i) Cu(II)-assisted Friedel-Crafts pathway. For this pathway the reaction starts with the coordination of Cu(II) with the substrate. After coordination, the Cu(II) complex **O-Int1** isomerizes to an active precursor **O/FC-Int1-II** which can cause an electrophilic attack through the transition state **O/FC-TS12-II** with an activation energy of +48.8

kcal/mol (Figure 4). This electrophilic attack leads to the intermediate **O/FC-Int2-II** and a reduced Cu(0) species. After removal of the reduced Cu(0) from **O/FC-Int2-II**, rearomatization takes place via the triflate-assisted deprotonation transition state **O/FC-TS23-II**. Then HOTf is released to generate benzoxazole as the final product. Meanwhile Cu(0) is re-oxidized to Cu(II). Note that the rate-limiting step of the above process is deprotonation with an overall activation energy of +49.8 kcal/mol. This barrier is too high for the reaction to proceed at the reported temperature (140 °C).

(ii) Cu(III)-assisted Friedel-Crafts pathway. As discussed above, the active Cu(III) complex **O/CMD-Int1-III** can also be generated in the system through oxidation. After oxidation, the Cu(III)-bound O atom in **O/CMD-Int1-III** can react with the aromatic ring through electrophilic attack (Figure 5). A Cu(I) intermediate, i.e. **O/FC-Int2-III-1**, is

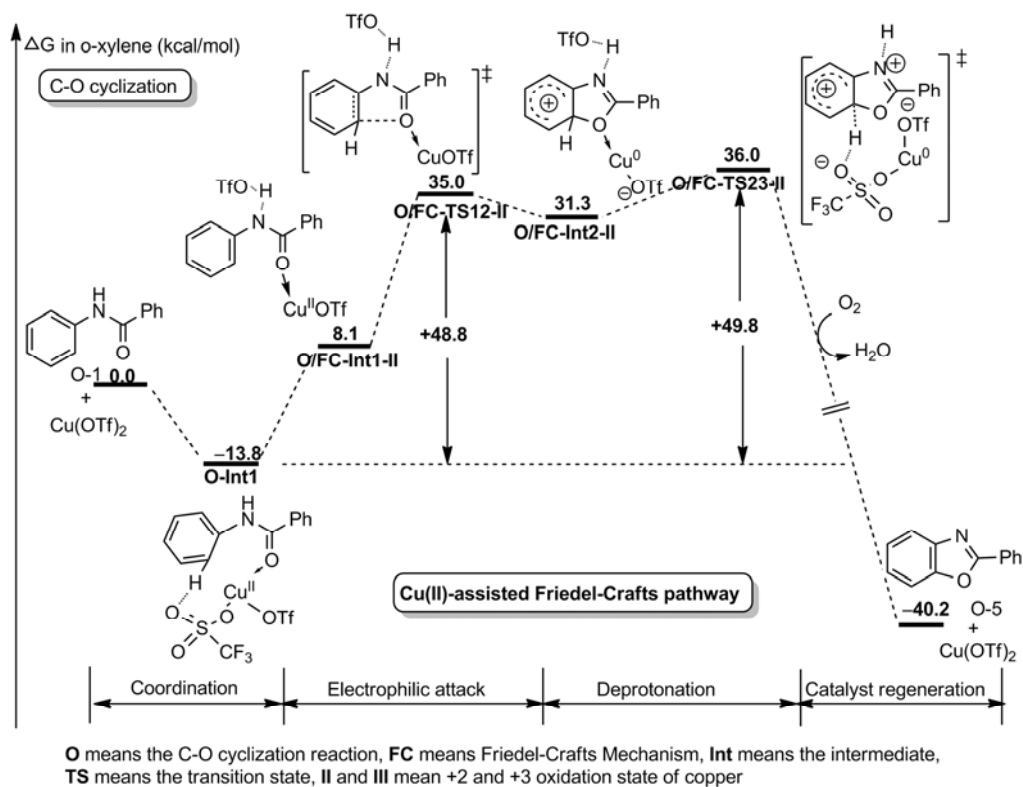


**Figure 4** Cu(II)-assisted Friedel-Crafts pathway for C–O formation.

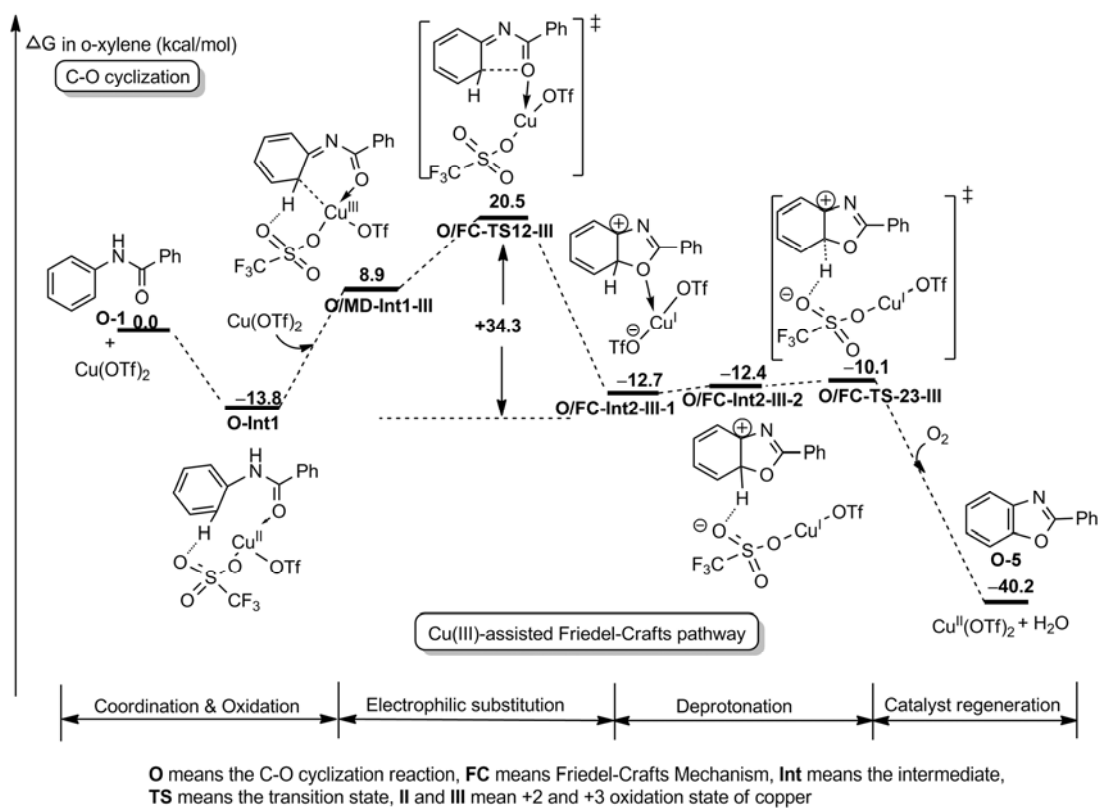


**Figure 5** Cu(III)-assisted Friedel-Crafts pathway in C–O formation.

then generated, which can undergo deprotonation readily through the transition state **O/FC-TS23-III**. Finally, HOTf is released to generate benzoxazole as the final product. Meanwhile Cu(I) is re-oxidized to Cu(II). In the above process, the rate-determining step is electrophilic attack and the overall barrier is +34.3 kcal/mol. This barrier is lower than that for Cu(II)-assisted Friedel-Crafts pathway, but is still higher than that for Cu(II)-assisted CMD mechanism.

#### 2.1.4 Comparing different pathways in C–O formation

To summarize the above calculations, the energy profiles for different mechanisms of Cu-catalyzed *ortho*-C–H activation/C–O formation are shown in Figure 6. According to these profiles, Cu(II)-assisted CMD pathway is favored as compared to its Cu(III) counterpart. It is also more favorable than either Cu(II)- or Cu(III)-assisted Friedel–Crafts pathway. This Cu(II)-assisted CMD pathway consists of three steps, i.e. concerted metalation–deprotonation with Cu(II), oxidation of the Cu(II) intermediate, and reductive elimination from Cu(III). The overall barrier is +31.6 kcal/mol and the rate-limiting step is reductive elimination from Cu(III) to generate the C–O bond.

## 2.2 Mechanism for C–N cyclization

Just as for the C–O cyclization of amides, Cu-catalyzed *ortho*-C–H activation/C–N cyclization of amidines may proceed via either B or C mechanism with +2 or +3 oxidation states of Cu [8, 25]. Based on our calculations, we also find that the Cu(II)-assisted CMD pathway is favored over

its Cu(III) counterpart and Cu(II)/Cu(III)-assisted Friedel–Crafts pathways [26] (Figure 7).

The Cu(II)-assisted CMD pathway also consists of three steps in the C–N cyclization, i.e. concerted metalation–deprotonation with Cu(II), oxidation of the Cu(II) intermediate, and reductive elimination from Cu(III). As Figure 8 shows, the imine moiety in the substrates can coordinate with the catalyst Cu(OAc)<sub>2</sub> to provide a stable Cu(II) complex **N-Int1** (exergonic, –4.8 kcal/mol). The Cu(II) center of **N-Int1** then attacks the N-phenyl ring via the six-membered-ring transition state **N/CMD-TS12-II**. This process is a CMD process involving the breaking of the CPh–H bond and concerted formation of C–Cu bond. After this CMD process, a new four-coordinated Cu(II) complex **N/CMD-Int2-II-1** is obtained which then may be oxidized to a Cu(III) intermediate **N/CMD-Int2-III-2**. Subsequently, **N/CMD-Int2-III-2** undergoes reductive elimination to give the product. This process shows a barrier of +13.2 kcal/mol (from **N/CMD-Int2-II-1** to **N/CMD-TS23-III**).

Different from C–O cyclization reaction, the concerted metalation–deprotonation step is the rate-limiting step for the C–N cyclization. The overall activation energy for the C–N cyclization is +22.0 kcal/mol.

Note that the overall energy barrier of the C–N cyclization (+22.0 kcal/mol) is lower than that of the C–O cyclization (+31.6 kcal/mol). This result is consistent with the experiments that the C–N cyclization can be carried out under milder conditions than the C–O cyclization (100 °C for the former versus 140 °C for the latter). Nonetheless, we believe that the energy barrier for the C–N cyclization (+22.0

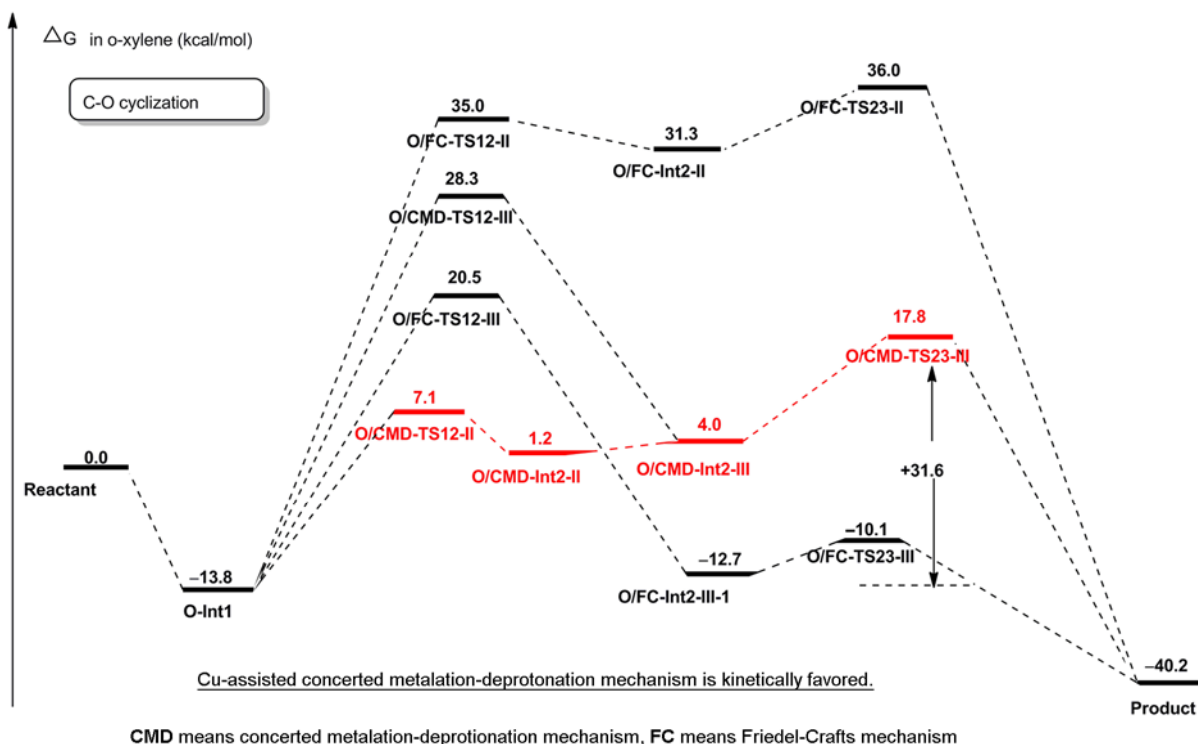


**Figure 6** Comparison of the energy profiles of mechanisms of Cu-catalyzed *ortho*-C–H activation/C–O cyclization reactions.

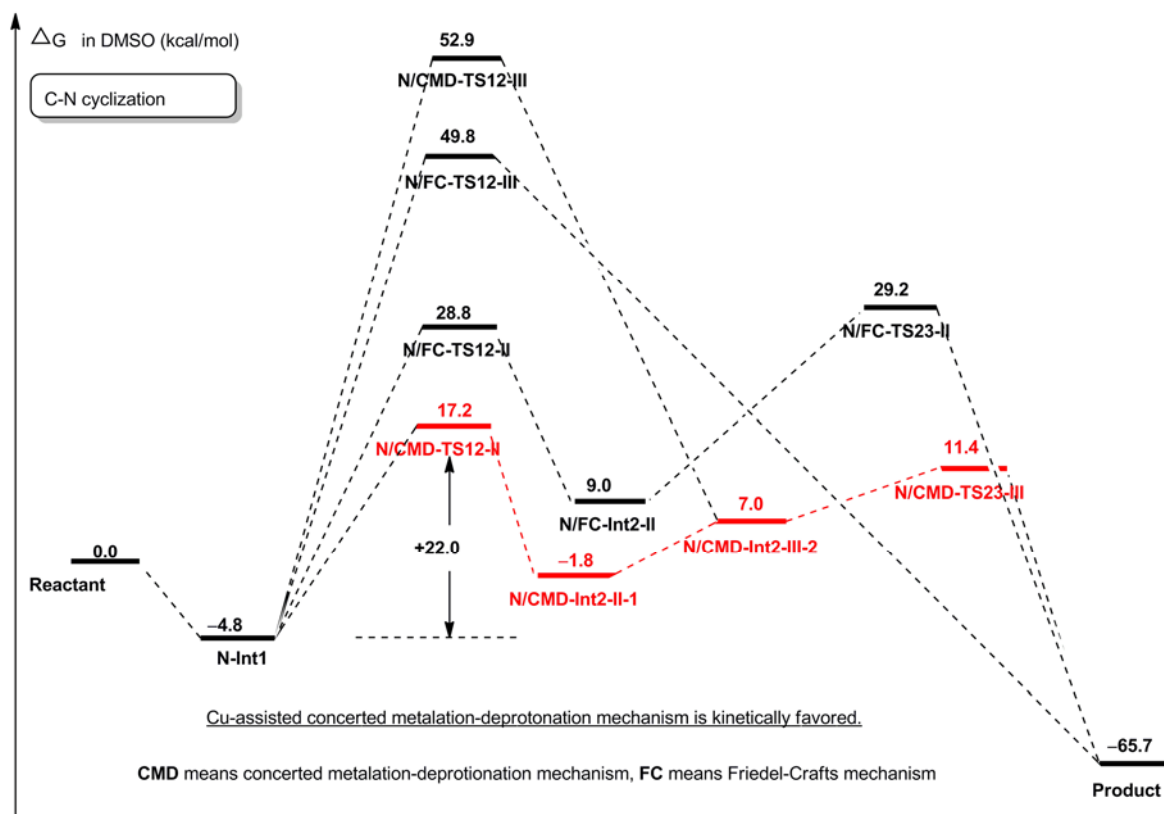


**Figure 7** Comparison of the energy profiles of mechanisms of Cu-catalyzed *ortho*-C–H activation/C–N cyclization reactions.

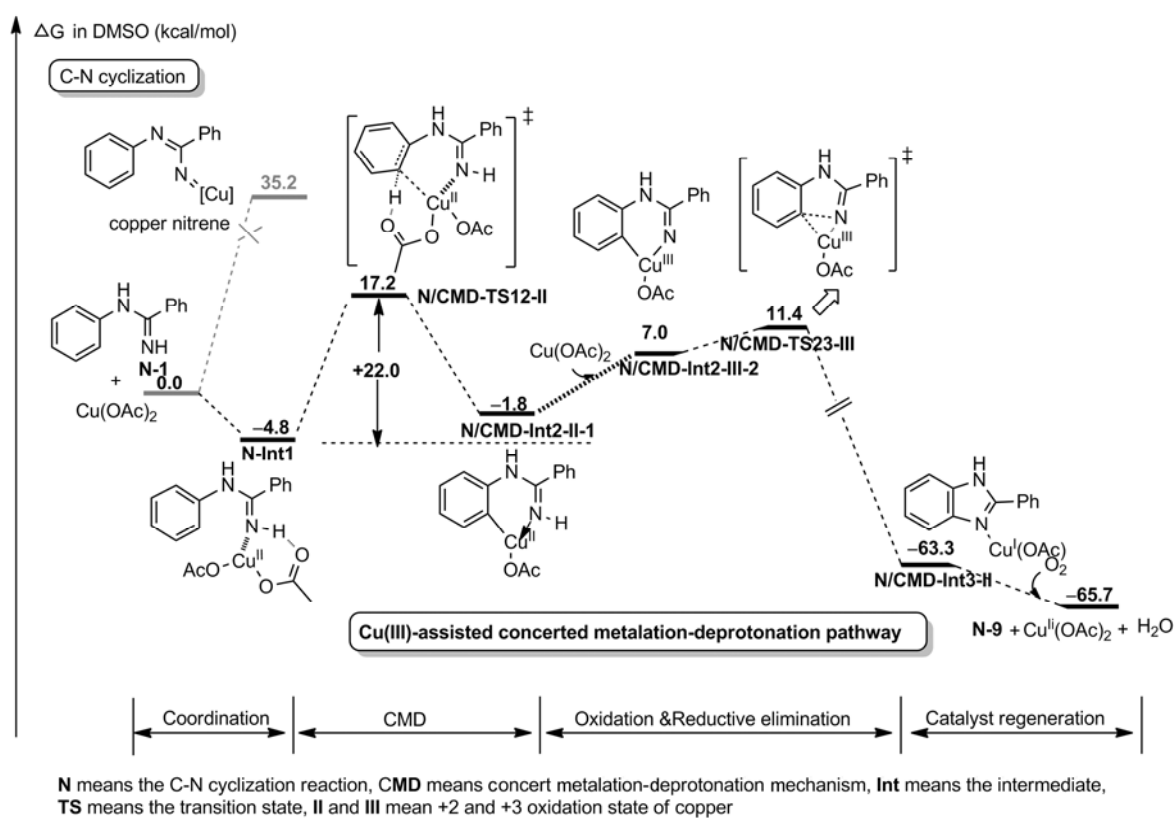


**Figure 8** Cu(II)-assisted concerted metalation–deprotonation pathway in C–N formation. Details of other disfavored pathways (Cu(II)/Cu(III)-assisted Friedel–Craft pathways and Cu(III)-assisted CMD pathway) are shown in the Supporting Information.

kcal/mol) is underestimated to some extent. The reason is that we assume that the reactants of the C–N cyclization are compound **N-1** and free  $\text{Cu}(\text{OAc})_2$ . Due to the strong binding ability of acetate anion,  $\text{Cu}(\text{OAc})_2$  may exist as clusters (i.e.  $\text{Cu}_n(\text{OAc})_{2n}$ ) so that the effective concentration of  $\text{Cu}(\text{OAc})_2$  may be much lower than theoretically assumed. This effect is difficult to estimate by current theoretical methods, but it means that the energy barrier is underestimated by our calculations.

### 2.3 Problems with the radical mechanisms

The radical mechanism via single electron transfer was previously proposed by Yu *et al.* to explain  $\text{Cu}(\text{OAc})_2$ -catalyzed pyridine-directed *ortho*-C–H functionalization [7a, 27]. Moreover, Stahl *et al.* suggested that the radical pathway should be considered for a related reaction [5b]. Despite these proposals, there has been no experimental test of the involvement of radical pathways for the C–N and C–O cyclizations shown in Scheme 1.

To solve this problem, we performed the reactions (Table 1) with radical scavengers. Considering Cu-mediated intermolecular C–X (X = N, O) coupling as side reactions, the commonly used radical scavengers containing N or O atom (i.e. 2, 2, 6, 6-tetramethylpiperidine-1-oxyl (TEMPO) or galvinoxyl) were not used. We noticed that Thomas *et al.* previously ruled out the radical mechanism for the Cu-mediated Ullmann arylation by showing that the reactions was not quenched by 1, 1-diphenylethylene [18b]. Here, for the Cu-catalyzed intramolecular C–H activation, we examined the effect of adding 1, 1-diphenylethylene (Table 1) [18b]. The yields of benzoxazole and benzimidazole were 54 [28] and 41%, respectively. Similarly, the reactions in

the presence of 1, 4-cyclohexadiene (which is another effective radical trapper used by Sanford *et al.*) [29] afforded the products in 60 [28] and 44% yields, respectively (Table 1). The results indicate that the reactions are not inhibited by the radical scavengers.

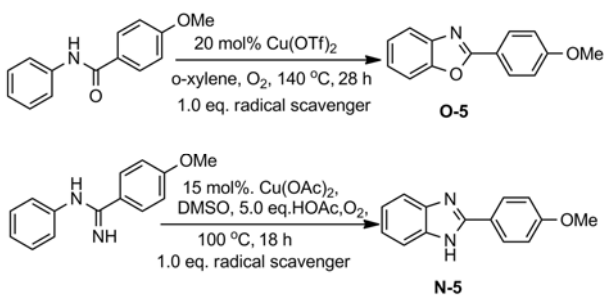
In addition, we tried to calculate the important intermediate **O-6**, an arene radical species in a single electron transfer route. In theory **O-6** and **O-Int1** could not be compared in energy because they have the same geometry as **O-2-II** shown in Scheme 5. The difference between **O-Int1** and **O-6** is the aromaticity of ring1 and thus we calculated the spin density of **O-2-II** to distinguish two species. The total spin density observed over the six C atoms of ring1 is 0.007 electron (1 electron for the molecule **O-2-II**). Moreover, the HOMA index of ring1 is 0.999 (0.994 for the amide **O-1**). These data both suggest that the ring1 must possess aromaticity, which is consistent with the Cu(II) complex **O-Int1** rather than the arene radical species **O-6**. Without the existence of the arene radical species, the single electron transfer is not plausible.

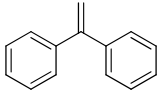
We also calculate the free energy of the proposed radical intermediates (**O-8** or **N-8** [30]) (Scheme 6). It is found that the formation of **O-8** and **N-8** from their Cu-bound precursors is highly endergonic (+55.1 and +32.5 kcal/mol, respectively). Consequently, the activation energies for generation of **O-8** and **N-8** must be higher than +55.1 and +32.5 kcal/mol, again indicating that the radical process is not feasible under the reaction conditions.

### 2.4 Problems with proton-coupled electron transfer

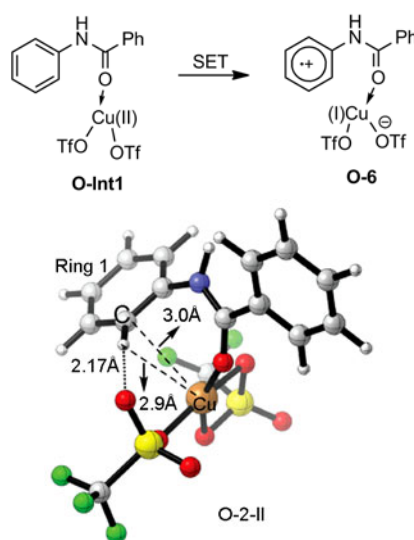
Ribas *et al.* reported in 2010 that proton-coupled electron transfer (PCET) could occur in Cu-mediated C–H cleavage reactions in the presence of special macrocyclic ligands [10]. They revealed that the C–H...Cu(II) interaction is a vital fea-

**Table 1** Effects of radical scavengers on the reaction efficiency

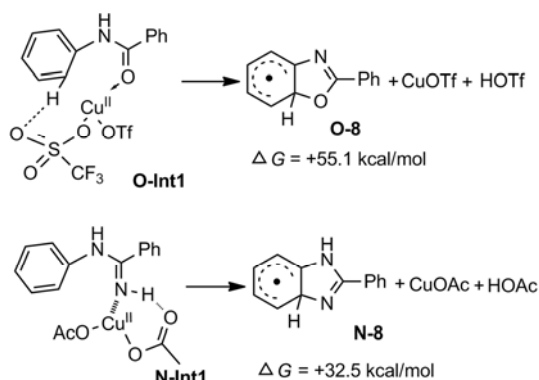


| Entry | Radical scavenger   | Yield <sup>a)</sup> of <b>O-5</b> (%) | Yield <sup>a)</sup> of <b>N-5</b> (%) |
|-------|---|---------------------------------------|---------------------------------------|
| 1     | –   | 81 (89 <sup>b)</sup> )                | 45 <sup>c)</sup>                      |
| 2     |  | 54                                    | 41                                    |
| 3     |  | 60                                    | 44                                    |

a) Isolated yield; b) yield in the literature [9a]; c) the substrate is not involved in Buchwald's reaction [8].



**Scheme 5** The structure of **O-2-II** is best described as **O-Int1**, rather than **O-6**.



**Scheme 6** Free energies for the formation of proposed radical intermediates.

ture of the PCET pathway. However, in the present study, with the aid of OAc/OTf, the C–H···Cu(II) distance is 2.90 Å, much longer than 2.14 Å in the reaction reported by Ribas. Thus, the proton-coupled electron transfer with unimolecular Cu-catalyst does not appear possible in the Buchwald's and Nagasawa's reactions.

Moreover, we also considered the PCET pathway involving bimolecular Cu-catalysts. In such pathway, another Cu(OAc)<sub>2</sub> molecule abstracts the H from the substrate and at the same time the extra Cu(II) center is reduced by one electron. In other words, the CMD and oxidation take place simultaneously with the help of another molecule of Cu catalyst. We only calculated the transition state (N/PCET-TS12) of this pathway in Buchwald's C–N coupling reaction, because in Buchwald's reaction the cleavage of C–H bond is the rate-determining step. The free energy of N/PCET-TS12 is +48.9 kcal/mol, which is much higher than that of N/CMD-TS12-II (+17.2 kcal/mol) in the CMD path-

way. Therefore, the PCET with a bimolecular Cu-catalyst is not plausible, either.

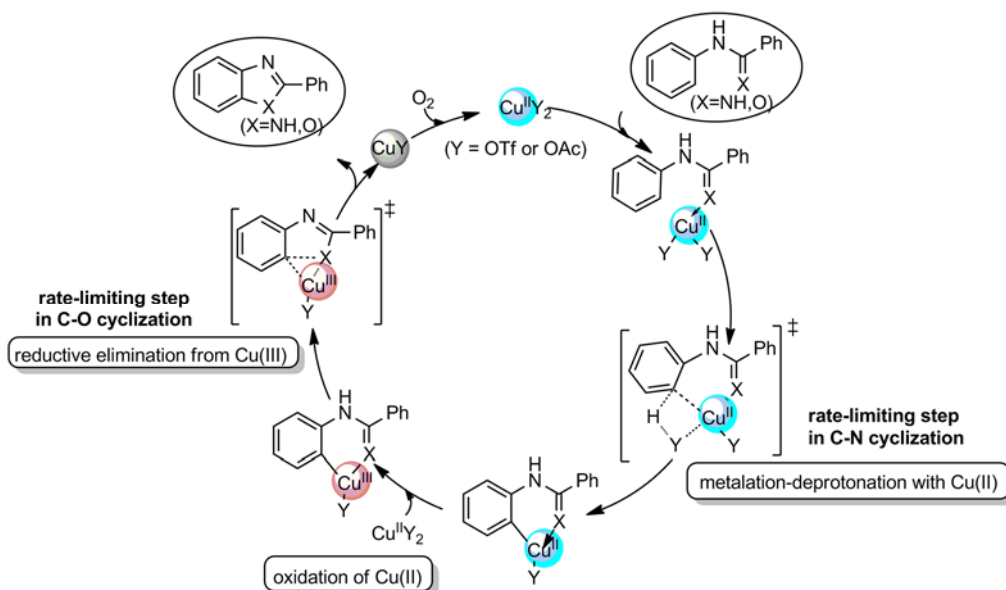
### 3 Comparisons with the experiments

The above theoretical calculations show that Cu(II)-assisted CMD pathway is energetically favored in both the *ortho*-C–H activation/C–O and C–N cyclization reactions. Such pathway proceeds through three steps: concerted metalation-deprotonation with Cu(II), oxidation of Cu(II) intermediate, and reductive elimination from Cu(III) (Scheme 7). However, in the case of C–O cyclization reductive elimination is the rate-limiting step, whereas in C–N cyclization concerted metalation-deprotonation is the rate-limiting step. Below we use some experimental results to test these theoretical proposals.

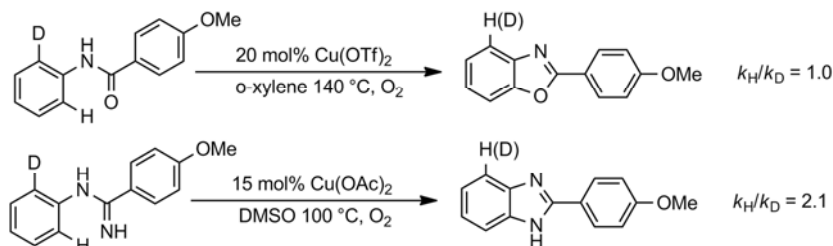
#### 3.1 Kinetic isotope effects

Because concerted metalation-deprotonation (i.e. C–H activation) is the rate-limiting step in C–N but not in C–O cyclization, we expect to see different kinetic isotope effects (KIE) in the two cyclizations reactions. In the case of C–O cyclization, Nagasawa *et al.* previously determined the KIE value to be 1.0 [9a], which is in good agreement with our theory.

No KIE study has been reported for C–N cyclization reaction. Thus we measure the intramolecular kinetic isotope effect using the *ortho*-deuterium labeled substrate (Scheme 8). The ratio of the *ortho*-proton product versus the *ortho*-deuterium product is 2.1:1.0. Thus the C–N cyclization reaction exhibits a KIE that is different from the C–O cyclization. This result verifies our theoretical prediction



**Scheme 7** Proposed mechanism of Cu-catalyzed *ortho*-C–H activation/C–N and C–O cyclizations.



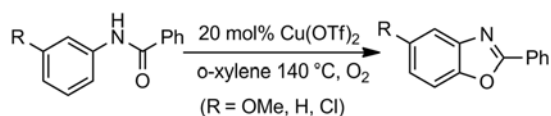
**Scheme 8** Intramolecular kinetic isotope effect.

that the C–H bond activation is the rate-limiting step for C–N coupling.

### 3.2 Substituent effects

Nagasawa and Buchwald previously examined the reactions with different substituents (Schemes 9 and 10). They found that the reaction with an electron-donating substituent ( $R = \text{OMe}$ ) is faster than that with an electron-withdrawing group ( $R = \text{Cl}$  or  $\text{COOMe}$ ). These observations were used to support the hypothesis that the C–N/C–O cyclization occurs via an electrophilic attack mechanism [8, 9].

Here we calculate the energy barriers for the reactions with electron-donating OMe and electron-withdrawing Cl or COOMe groups on the basis of the proposed mechanism (i.e. the Cu(II)-assisted CMD pathway). It is found that for C–O cyclization, the energy barriers are +31.4, +31.6 and +33.0 kcal/mol for OMe, H and Cl substituted substrates. Thus the reactivity of substituted amides decreases in the order:  $\text{OMe} > \text{H} > \text{Cl}$ . This calculated trend is consistent with experiment. As to C–N cyclization, the energy barriers are calculated to be +21.1, +22.0 and +22.7 kcal/mol for OMe, H and COOMe substituted substrates, respectively. Thus the

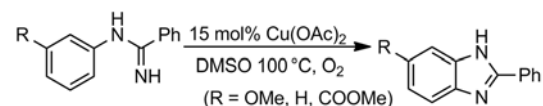


Experiment:  $k_{(R=\text{OMe})} > k_{(R=\text{H})} > k_{(R=\text{Cl})}$

Calculation:  $\Delta G^\ddagger_{(R=\text{OMe})}(+31.4) < \Delta G^\ddagger_{(R=\text{H})}(+31.6) < \Delta G^\ddagger_{(R=\text{Cl})}(+33.0)$

Unit: kcal/mol

**Scheme 9** Substituent effects on Cu-catalyzed C–H activation/C–O cyclization.



Experiment:  $k_{(R=\text{OMe})} > k_{(R=\text{H})} > k_{(R=\text{COOMe})}$

Calculation:  $\Delta G^\ddagger_{(R=\text{OMe})}(+21.1) < \Delta G^\ddagger_{(R=\text{H})}(+22.0) < \Delta G^\ddagger_{(R=\text{COOMe})}(+22.7)$

Unit: kcal/mol

**Scheme 10** Substituent effects on Cu-catalyzed C–H activation/C–N cyclization.

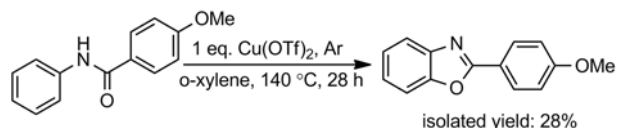
reactivity of substituted amidines decreases in the order:  $\text{OMe} > \text{H} > \text{COOMe}$ . This calculated trend is also consistent with experiment, thus supporting the mechanism proposed in Scheme 7.

### 3.3 O<sub>2</sub>-free reactions

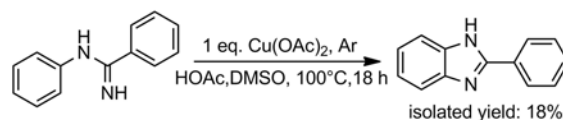
According to the mechanism in Scheme 7, the generation of the active Cu(III) species does not require the involvement of  $\text{O}_2$ . Instead,  $\text{O}_2$  is needed for the catalyst regeneration step. If this proposal is correct, we must be able to observe that the reaction can proceed to some extent without addition of  $\text{O}_2$ . Indeed, when we carried out the same C–O and C–N cyclization reactions in under Ar protection using Schlenk techniques (Schemes 11 and 12), moderate isolated yields of 28% and 18% were obtained for the C–O and C–N cyclization products (theoretically, yields of the reaction should be 50% in the presence of 1 equivalent of Cu salts and the decrease in yield can be attributed to unknown side-reactions suppressed by  $\text{O}_2$ ). These results confirm that the active Cu(III) species can be generated via disproportionation in the absence of  $\text{O}_2$ .

## 4 Conclusions

Cu-catalyzed C–H functionalization has recently attracted considerable interest. In the present study, we report a comprehensive theoretical study (together with some experimental tests) of the mechanism of the Cu-catalyzed intramolecular *ortho*-C–H activation/C–O and C–N cyclization



**Scheme 11** O<sub>2</sub>-free C–H activation/C–O cyclization of amides.



**Scheme 12** O<sub>2</sub>-free C–H activation/C–N cyclization of amidines.

reactions. By comparing the CMD and Friedel–Crafts mechanisms with different oxidation states of Cu (+2, +3), we find that the Cu(II)-assisted concerted metalation-deprotonation (CMD) pathway is the most favorable for both the C–O and C–N cyclization reactions. The Cu(II)-assisted CMD mechanism consists of three steps, i.e. concerted metalation-deprotonation with Cu(II), oxidation of the Cu(II) intermediate, and reductive elimination from Cu(III). In particular, it is the Cu(II) species that mediates the C–H activation process through an OAc/OTf-assisted six-membered-ring CMD transition state similar to that proposed for many Pd-catalyzed C–H activation reactions. Also interestingly, while the rate-determining step in the C–O cyclization reaction is reductive elimination, the rate-determining step in the C–N cyclization reaction is the concerted metalation–deprotonation step. This finding is consistent with the experimental kinetic isotope effects (1.0 and 2.1 for C–O and C–N cyclization reactions, respectively). We also show that the proposed mechanism is consistent with the experimental substituent effects. Finally, we carry out reactions under O<sub>2</sub>-free conditions and verify that the Cu(III)-formation step can proceed without O<sub>2</sub>.

## 5 Computational methods and experimental details

### 5.1 Computational methods

Geometry optimization of all compounds in the gas phase without any constraint was conducted by the density functional theory method B3P86 [31] with the basis set 6-31+G(d) [32]. This method has been successfully used in many recent studies to study the mechanism of transition metal-catalyzed reactions [10, 33, 34]. Frequency calculations were conducted at the same level of theory as geometry optimization to confirm whether the stationary points were minima or saddle points. For saddle points, intrinsic reaction coordinate (IRC) analysis [35] was performed to verify that they connect the right reactants and products on the potential energy surface. Single-point energy calculations were performed by using the M06 method [36] with a more flexible basis set 6-311++G(d, p). Note that this method was recently used by Yates *et al.* to study Cu-mediated carboxylation reaction [37]. The solvent effect was calculated with a self-consistent reaction field (SCRF) method using the SMD model [31a, 38]. *o*-Xylene ( $\epsilon = 2.545$ ) and dimethyl sulfoxide (DMSO) ( $\epsilon = 46.826$ ) used in the experiments were directly calculated. All the calculations were performed with the Gaussian09 suite [39] of programs. Single-point energies in the solution corrected by the Gibbs free energy correction from frequency calculations were conducted to describe the reaction energetics throughout the study. All the solution-phase free energies presented in the work correspond to the reference state of 1 mol/L, 298K.

### 5.2 General procedure for Cu-catalyzed *ortho*-C–H activation/C–O cyclization

To a Schlenk tube was added **O-1** (0.25 mmol) and Cu(OTf)<sub>2</sub> (0.05 mmol). The tube was evacuated and back-filled with O<sub>2</sub> (or without O<sub>2</sub> for O<sub>2</sub>-free reactions). Then *o*-xylene (0.5 mL) was added via syringe. Note that the radical scavenger (0.25 mmol) was added for the radical scavenger experiment. The reaction mixture was put into a preheated oil bath at 140 °C and stirred for 28 h. Subsequently a small amount of ethyl acetate was added and the residue was purified by silica gel chromatography. NMR spectra are shown in the Supporting Information.

### 5.3 General procedure for Cu-catalyzed *ortho*-C–H activation/C–N cyclization

To a Schlenk tube was added **N-1** (0.25 mmol) and Cu(OAc)<sub>2</sub> (0.0375 mmol). The tube was evacuated and backfilled with O<sub>2</sub> (or without O<sub>2</sub> for O<sub>2</sub>-free reaction). Then HOAc (2.5 mmol, 5.00 equiv.), and DMSO (0.5 mL) was added by syringe. Note that the radical scavenger (0.25 mmol) was added for the radical scavenger experiments. The reaction mixture was put into a preheated oil bath at 100 °C and stirred for 18 h. Subsequently a small amount of ethyl acetate was added and the residue was purified by silica gel chromatography. NMR spectra are shown in the Supporting Information.

*We are grateful for the financial support from the National Basic Research Program of China (973 program, 2012CB215306), the National Natural Science Foundation of China (NSFC, 20832004, 20972148) and CAS (KJCX2-EW-J02). The numerical calculations in this paper were carried out on the supercomputing system in the Supercomputer Center of University of Science and Technology of China.*

- 1 Balcells D, Clot E, Eisenstein O. C–H bond activation in transition metal species from a computational perspective. *Chem Rev*, 2010, 110: 749–823
- 2 Colby DA, Bergman RG, Ellman JA. Rhodium-catalyzed C–C bond formation via heteroatom-directed C–H bond activation. *Chem Rev*, 2010, 110: 624–655
- 3 Collet F, Lescot C, Dauban P. Catalytic C–H amination: The stereoselectivity issue. *Chem Soc Rev*, 2011, 40: 1926–1936
- 4 a) Lyons TW, Sanford MS. Palladium-catalyzed ligand-directed C–H functionalization reactions. *Chem Rev*, 2010, 110: 1147–1169; b) Xu LM, Li BJ, Yang Z, Shi ZJ. Organopalladium(IV) chemistry. *Chem Soc Rev*, 2010, 39: 712–733; For recent examples, see: c) Wang DH, Engle KM, Shi BF, Yu JQ. Ligand-enabled reactivity and selectivity in a synthetically versatile aryl C–H olefination. *Science*, 2010, 327: 315–319; d) Mandal D, Yamaguchi AD, Yamaguchi J, Itami K. Synthesis of drarmacidin D via direct C–H couplings. *J Am Chem Soc*, 2011, 133: 19660–19663; e) Xiao B, Gong TJ, Liu ZJ, Liu JH, Luo DF, Xu J, Liu L. Synthesis of dibenzofurans via palladium-catalyzed phenol-directed C–H activation/C–O cyclization. *J Am Chem Soc*, 2011, 133: 9250–9253; f) Xiao B, Gong TJ, Xu J, Liu ZJ, Liu L. Palladium-catalyzed intermolecular directed C–H amidation of aromatic ketones. *J Am Chem Soc*, 2011, 133: 1466–1474; g) Ueda K, Yanagisawa S, Yamaguchi J, Itami K. A general catalyst for the  $\beta$ -selective C–H bond arylation of thiophenes with iodoarenes.

- Angew Chem Int Ed*, 2010, 49: 8946–8949; h) Dai HX, Yu JQ. Pd-catalyzed oxidative *ortho*-C–H borylation of arenes. *J Am Chem Soc*, 2012, 134: 134–137; i) Wasa M, Engle KM, Lin DW, Yoo EJ, Yu JQ. Pd(II)-catalyzed enantioselective C–H activation of cyclopropanes. *J Am Chem Soc*, 2011, 133: 19598–19601
- 5 a) Wendlandt AE, Suess AM, Stahl SS. Copper-catalyzed aerobic oxidative C–H functionalizations: Trends and mechanistic insights. *Angew Chem Int Ed*, 2011, 50: 11062–11087; b) Yang L, Lu Z, Stahl SS. Regioselective copper-catalyzed chlorination and bromination of arenes with O<sub>2</sub> as the oxidant. *Chem Commun*, 2009, 6460–6462
- 6 a) Li Z, Bohle DS, Li CJ. Cu-catalyzed cross-dehydrogenative coupling: A versatile strategy for C–C bond formations via the oxidative activation of sp(3) C–H bonds. *Proc Natl Acad Sci U S A*, 2006, 103: 8928–8933; b) Do HQ, Daugulis O. Copper-catalyzed arylation of heterocycle C–H bonds. *J Am Chem Soc*, 2007, 129: 12404–12405; c) Do HQ, Daugulis O. Copper-catalyzed arylation and alkenylation of polyfluoroarene C–H bonds. *J Am Chem Soc*, 2008, 130: 1128–1129
- 7 Chen X, Hao XS, Goodhue CE, Yu JQ. Cu(II)-catalyzed functionalizations of aryl C–H bonds using O<sub>2</sub> as an oxidant. *J Am Chem Soc*, 2006, 128: 6790–6791
- 8 Brasche G, Buchwald SL. C–H functionalization/C–N bond formation: Copper-catalyzed synthesis of benzimidazoles from amidines. *Angew Chem Int Ed*, 2008, 47: 1932–1934
- 9 a) Ueda S, Nagasawa H. Synthesis of 2-arylbenzoxazoles by copper-catalyzed intramolecular oxidative C–O coupling of benzanilides. *Angew Chem Int Ed*, 2008, 47: 6411–6413; b) Ueda S, Nagasawa H. Copper-catalyzed synthesis of benzoxazoles via a regioselective C–H functionalization/C–O bond formation under an air atmosphere. *J Org Chem* 2009, 74: 4272–4277
- 10 Ribas X, Calle C, Poater A, Casitas A, Gomez L, Xifra R, Parella T, Benet-Buchholz J, Schweiger A, Mitrikas G, Sola M, Llobet A, Stack TD. Facile C–H bond cleavage via a proton-coupled electron transfer involving a C–H...Cu(II) interaction. *J Am Chem Soc*, 2010, 132: 12299–12306
- 11 a) Yao B, Wang DX, Huang ZT, Wang MX. Room-temperature aerobic formation of a stable aryl–Cu(III) complex and its reactions with nucleophiles: Highly efficient and diverse arene C–H functionalizations of azacalix[1]arene[3]pyridine. *Chem Commun*, 2009, 2899–2901; b) Wang ZL, Zhan L, Wang MX. Regiospecific functionalization of azacalixaromatics through copper-mediated aryl C–H activation and C–O bond formation. *Org Lett*, 2011, 13: 6560–6563
- 12 a) Huffman LM, Casitas A, Font M, Canta M, Costas M, Ribas X, Stahl SS. Observation and mechanistic study of facile C–O bond formation between a well-defined aryl-copper(III) complex and oxygen nucleophiles. *Chem Eur J*, 2011, 17: 10643–10650; b) Huffman LM, Stahl SS. Carbon-nitrogen bond formation involving well-defined aryl-copper(III) complexes. *J Am Chem Soc*, 2008, 130: 9196–9197
- 13 Garcia-Lopez J, Yanez-Rodriguez V, Roces L, Garcia-Granda S, Martinez A, Guevara-Garcia A, Castro GR, Jimenez-Villacorta F, Iglesias MJ, Lopez Ortiz F. Synthesis and characterization of a coupled binuclear Cu(I)/Cu(III) complex. *J Am Chem Soc*, 2010, 132: 10665–10667
- 14 a) Chen B, Hou XL, Li YX, Wu YD. Mechanistic understanding of the unexpected meta selectivity in copper-catalyzed anilide C–H bond arylation. *J Am Chem Soc*, 2011, 133: 7668–7671; b) Wang M, Fan T, Lin Z. DFT Studies on copper-catalyzed arylation of aromatic C–H Bonds. *Organometallics*, 2012, 31: 560–569; c) Santoro S, Liao RZ, Himmo F. Theoretical study of mechanism and selectivity of copper-catalyzed C–H bond amidation of indoles. *J Org Chem*, 2011, 76: 9246–9252
- 15 a) Gorelsky SI, Lapointe D, Fagnou K. Analysis of the concerted metalation–deprotonation mechanism in palladium-catalyzed direct arylation across a broad range of aromatic substrates. *J Am Chem Soc*, 2008, 130: 10848–10849; b) Garcia-Cuadrado D, Mendoza P De; Braga AAC, Maseras F, Echavarren AM. Proton-abstraction mechanism in the palladium-catalyzed intramolecular arylation: Substituent effects. *J Am Chem Soc*, 2007, 129: 6880–6886
- 16 a) Kruszewski J, Krygowski TM. Definition of aromaticity Basing on the harmonic oscillator model. *Tetrahedron Lett*, 1972, 13: 3839–3842; b) Krygowski TM, Cyranski MK. Structural aspects of aromaticity. *Chem Rev*, 2001, 101: 1385–1419
- 17 NICS(1) estimated at 1A above the center of the ring. For details see: Schleyer PvR, Maerker C, Dransfeld A, Jiao H, van Eikema Hommes NJR. Nucleus-independent chemical shifts: A simple and efficient aromaticity probe. *J Am Chem Soc*, 1996, 118: 6317–6318
- 18 a) Yu HZ, Jiang YY, Fu Y, Liu L. Alternative mechanistic explanation for ligand-dependent selectivities in copper-catalyzed N- and O-arylation reactions. *J Am Chem Soc*, 2010, 132: 18078–18091; b) Zhang SL, Liu L, Fu Y, Guo QX. Theoretical study on copper(I)-catalyzed cross-coupling between aryl halides and amides. *Organometallics*, 2007, 26: 4546–4554
- 19 Casitas A, King AE, Parella T, Costas M, Stahl SS, Ribas X. Direct observation of Cu<sup>I</sup>/Cu<sup>III</sup> redox steps relevant to Ullmann-type coupling reactions. *Chem Sci*, 2010, 1: 326–330
- 20 Note that **O-Int1** is found to be the most stable. See Supporting Information for details.
- 21 a) Ribas X, Jackson DA, Donnadiou B, Mahia J, Parella T, Xifra R, Hedman B, Hodgson KO, Llobet A, Stack TDP. Aryl C–H activation by CuII to form an organometallic aryl–CuIII species: A novel twist on copper disproportionation. *Angew Chem Int Ed*, 2002, 41: 2991–2994; b) King AE, Brunold TC, Stahl SS. Mechanistic study of copper-catalyzed aerobic oxidative coupling of arylboronic esters and methanol: Insights into an organometallic oxidase reaction. *J Am Chem Soc*, 2009, 131: 5044–5045
- 22 Huffman LM, Casitas A, Font M, Canta M, Costas M, Ribas X, Stahl SS. Observation and mechanistic study of facile C–O bond formation between a well-defined aryl-copper(III) complex and oxygen nucleophiles. *Chem Eur J*, 2011, 17: 10642–10649
- 23 Sartori G, Maggi R. Use of solid catalysts in Friedel–Crafts acylation reactions. *Chem Rev*, 2006, 106: 1077–1104
- 24 Kuang GC, Guha PM, Brotherton WS, Simmons JT, Stanke LA, Nguyen BT, Clark RJ, Zhu L. Experimental investigation on the mechanism of chelation-assisted, copper(II) acetate-accelerated azide-alkyne cycloaddition. *J Am Chem Soc*, 2011, 133: 13984–14001
- 25 An alternative intermediate (i.e. Cu-nitrene may also be involved as proposed by Buchwald et al. for the C–N cyclization. However, our calculation shows that the formation of Cu-nitrene is highly endergonic (+35.2 kcal/mol) and therefore unfavorable (Figure 8).
- 26 For details about the disfavored routes, see Supporting Information.
- 27 Jones GO, Liu P, Houk KN, Buchwald SL. Computational explorations of mechanisms and ligand-directed selectivities of copper-catalyzed Ullmann-type reactions. *J Am Chem Soc*, 2010, 132: 6205–6213
- 28 In the case of C–O formation reaction with radical scavenger, the small decrease of yield is probably attributed to radical species or other alkene-promoted side-reactions. To further clarify the radical pathways, we calculated the important radical species **O-6** and **O-8**. The data suggested that the radical pathway might be not plausible.
- 29 Lanci MP, Remy MS, Kaminsky W, Mayer JM, Sanford MS. Oxidatively induced reductive elimination from ((t)Bu2bpy)Pd(Me)<sub>2</sub>: Palladium(IV) intermediates in a one-electron oxidation reaction. *J Am Chem Soc*, 2009, 131: 15618–15620
- 30 The wavefunction is stable under the perturbations considered.
- 31 a) Becke AD. Density-functional thermochemistry. III. The role of exact exchange. *J Chem Phys*, 1993, 98: 5648–5652; b) Perdew JP. Density-functional approximation for the correlation energy of the inhomogeneous electron gas. *J Phys Rev B*, 1986, 33: 8822–8824
- 32 Rassolov VA, Pople JA, Ratner MA, Windus TL. 6-31G\* basis set for atoms K through Zn. *J Chem Phys*, 1998, 109: 1223–1229
- 33 Pavelka M, Šimánek M, Šponer J, Burda JV. Copper cation interactions with biologically essential types of ligands: A computational DFT study. *J Phys Chem A*, 2006, 110: 4795–4809
- 34 a) Li Z, Fu Y, Zhang SL, Guo QX, Liu L. Heck-type reactions of imine derivatives: A DFT study. *Chem Asian J*, 2010, 5: 1475–1486; b) Shang R, Yang ZW, Wang Y, Zhang SL, Liu L. Palladium-catalyzed decarboxylative couplings of 2-(2-azaaryl)acetates with aryl halides and triflates. *J Am Chem Soc*, 2010, 132: 14391–14393; c) Zhang SL, Fu Y, Shang R, Guo QX, Liu L. Theoretical analysis of

- factors controlling Pd-catalyzed decarboxylative coupling of carboxylic acids with olefins. *J Am Chem Soc*, 2010, 132: 638–646; d) Shang R, Fu Y, Wang Y, Xu Q, Yu HZ, Liu L. Copper-catalyzed decarboxylative cross-coupling of potassium polyfluorobenzoates with aryl iodides and bromides. *Angew Chem Int Ed*, 2009, 48: 9350–9354; e) Li Z, Zhang SL, Fu Y, Guo QX, Liu L. Mechanism of Ni-catalyzed selective C–O bond activation in cross-coupling of aryl esters. *J Am Chem Soc*, 2009, 131:8815–8823
- 35 Gonzalez C, Schlegel HB. An Improved Algorithm for Reaction Path Following. *J Chem Phys*, 1989, 90: 2154–2161
- 36 Truhlar DG, Zhao Y. The M06 suite of density functionals for main group thermochemistry, thermochemical kinetics, noncovalent interactions, excited states, and transition elements: two new functionals and systematic testing of four M06-class functionals and 12 other functionals. *Theor Chem Acc*, 2008, 120: 215–241
- 37 Ariaifard A, Zarkoob F, Batebi H, Stranger R, Yates BF. DFT Studies on the carboxylation of the C–H bond of heteroarenes by copper(I) complexes. *Organometallics*, 2011, 30: 6218–6224
- 38 Cramer CJ, Marenich AV, Truhlar DG. Universal solvation model based on solute electron density and on a continuum model of the solvent defined by the bulk dielectric constant and atomic surface tensions. *J Phys Chem B*, 2009, 113: 6378–6396
- 39 Gaussian 09, Revision B.01, Frisch MJ, Trucks GW, Schlegel HB, et al. Wallingford CT: Gaussian Inc. 2010